Journal of Clinical & Experimental Cardiology

Koestenberger et al. J Clin Exp Cardiolog 2012, S:8
DOI: 10.4172/2155-9880.S8-002

Review Article Open Access

Non-Invasive Imaging for Congenital Heart Disease: Recent Innovations in Transthoracic Echocardiography

Martin Koestenberger[1]*, Mark K. Friedberg[2], William Ravekes[3], Eirik Nestaas[4] and Georg Hansmann[5,6]

[1]Division of Pediatric Cardiology, Department of Pediatrics, Medical University Graz, Austria
[2]The Labatt Family Heart Center, Hospital for Sick Children and University of Toronto, Toronto, Ontario, Canada
[3]Division of Pediatric Cardiology, Johns Hopkins University School of Medicine, Baltimore, MD, USA
[4]Department of Paediatrics, Oslo Vestfold Hospital Trust, Tønsberg, Norway
[5]Department of Cardiology, Children's Hospital Boston, Harvard Medical School, Boston, MA, USA
[6]Department of Pediatric Cardiology and Critical Care, Hannover Medical School, Hannover, Germany

Abstract

Transthoracic echocardiography (TTE) is an important tool for diagnosis and follow-up of patients with congenital heart disease (CHD). Appropriate use of TTE can reduce the need for more invasive and complex modalities, such as cardiac catheterization and cardiac magnetic resonance imaging. New echocardiographic techniques have emerged for the assessment of ventricular systolic and diastolic function: Tissue Doppler imaging, tissue tracking, strain and strain rate imaging, vector velocity imaging (VVI), myocardial performance index, myocardial acceleration during isovolumic contraction (IVA), the ratio of systolic to diastolic duration (S/D ratio), and other measurements of systolic right ventricular (RV) function like tricuspid annular plane systolic excursion (TAPSE). These modalities may become valuable indicators of ventricular performance, compliance and disease progression, with the caveat of preload-dependency of the variables measured. In addition, three-dimensional (3D) echocardiography for the assessment of cardiac anatomy, valvular function, device position, ventricular volumes and ejection fraction is integrated into routine clinical care. In this review, we discuss the potential use and limitations of these new echocardiographic techniques in patients with CHD. A particular focus is on the echocardiographic assessment of right ventricular (RV) function by means of tissue Doppler imaging, tissue tracking, and three-dimensional imaging, in conditions associated with increased right ventricular volume or pressure load.

Keywords: Tissue tracking; Speckle tracking; Vector velocity imaging; Tissue Doppler imaging; Strain; Strain rate; Isovolumic acceleration; Three-dimensional echocardiography; TAPSE

Abbreviations: ASD: Atrial Septal Defect; CHD: Congenital Heart Disease; CMP: Cardiomyopathy; EF: Ejection Fraction; ICT: Isovolumic Contraction Time; IRT: Isovolumic Relaxation Time; IVA: Isovolumic Acceleration; LV: Left Ventricle; MR: Mitral Regurgitation; MRI: Magnetic Resonance Imaging; PAH: Pulmonary Artery Hypertension; PR: Pulmonary Regurgitation; QRSd: QRS Duration; RV: Right Ventricle; RVEDVi: Indexed RV End-Diastolic Volume; S/D Duration: Systolic To Diastolic Duration; TAPSE: Tricuspid Annular Plane Systolic Excursion; TAPSV: Tricuspid Annular Peak Systolic Velocity; TDI: Tissue Doppler Imaging; TGA: Transposition Of The Great Arteries; TOF: Tetralogy Of Fallot; TR: Tricuspid Regurgitation; TTE: Transthoracic Echocardiography; VVI: Vector Velocity Imaging; 2D: Two-Dimensional; 3D: Three-Dimensional; HLHS: Hypoplastic Left Heart Syndrome

Introduction

Trans thoracic echocardiography (TTE) has become the most important and routinely applied non-invasive imaging technique for the diagnosis and follow-up of patients with congenital heart disease (CHD). Cross-sectional Doppler echocardiography allows a detailed description of cardiovascular anatomy, ventricular and valvular function. The diagnostic accuracy for describing cardiac morphology by TTE is very high, with a reported incidence of less than 100 errors in more than 50.000 echocardiograms [1]. Most functional variables used in echocardiography were developed and validated for the assessment of the normal, systemic, morphologically left ventricle (LV). The heterogeneity of CHD, anatomic normal variants, growth effects, and inter-study variability of hemodynamics complicate the proper interpretation of many functional variables. For the LV, adult techniques are often extrapolated to pediatrics without comprehensive validation in a large pediatric cohort or blinded prospective studies. For the RV, qualitative (subjective) assessment is the technique used routinely in most laboratories ("eye balling"). Right ventricular function is physiologically different than that of the LV, including different RV vs. LV myocardial arrangement [2-4], lower RV after load and lower systolic RV pressures compared with the LV.

Traditionally, dimensional changes or volumetric changes during systole of the cardiac cycle have been used to assess ventricular function. This can be done using M-mode techniques to measure fractional shortening or by volumetric techniques to calculate ejection fraction. These techniques are especially load-sensitive (preload dependent) and rely on geometrical assumptions. Therefore, they may not be readily applicable to congenital heart disease. Recent technical developments have renewed the interest in the assessment of ventricular performance in patients with CHD.

Newer techniques including tissue Doppler echocardiography, tissue tracking (speckle-tracking-based strain imaging), and vector velocity imaging (VVI) provide direct quantitative information

***Corresponding author:** Martin Koestenberger, MD, PhD, Department of Pediatrics, Medical University Graz, Auenbruggerplatz 30, A-8036 Graz, Austria, Tel: +43 316 385 2605; E-mail: Martin.Koestenberger@medunigraz.at

Received October 27, 2011; **Accepted** January 20, 2012; **Published** June 15, 2012

Citation: Koestenberger M, Friedberg MK, Ravekes W, Nestaas E, Hansmann G (2012) Non-Invasive Imaging for Congenital Heart Disease: Recent Innovations in Transthoracic Echocardiography. J Clin Exp Cardiolog S8:002. doi:10.4172/2155-9880.S8-002

about myocardial motion and deformation. Three-dimensional (3D-) echocardiographic techniques enable the acquisition of full volumetric datasets, which can be analysed offline for the calculation of ventricular volumes, mass and EF.

Transthoracic echocardiography has the advantage of lower cost, less risk, and greater availability compared with cardiac magnetic resonance imaging or cardiac catheterization. Transthoracic echocardiography remains the first line method for diagnosing congenital heart disease, particularly in young patients who usually have excellent imaging windows. In this review, we have not primarily focus on specific cardiovascular lesions but rather on emerging technologies, methods and variables, as they relate to myocardial contractility and function, and ventricular volumes including tissue Doppler imaging, tissue tracking and vector velocity imaging and deformation imaging for strain and strain rate, myocardial performance index, myocardial acceleration during isovolumic contraction (IVA) and the systolic to diastolic duration ratio. We also relate to measurements of longitudinal systolic RV function such as tricuspid annular plane systolic excursion (TAPSE) and peak systolic velocity (TAPSV), and 3D-echocardiography (Figure 1).

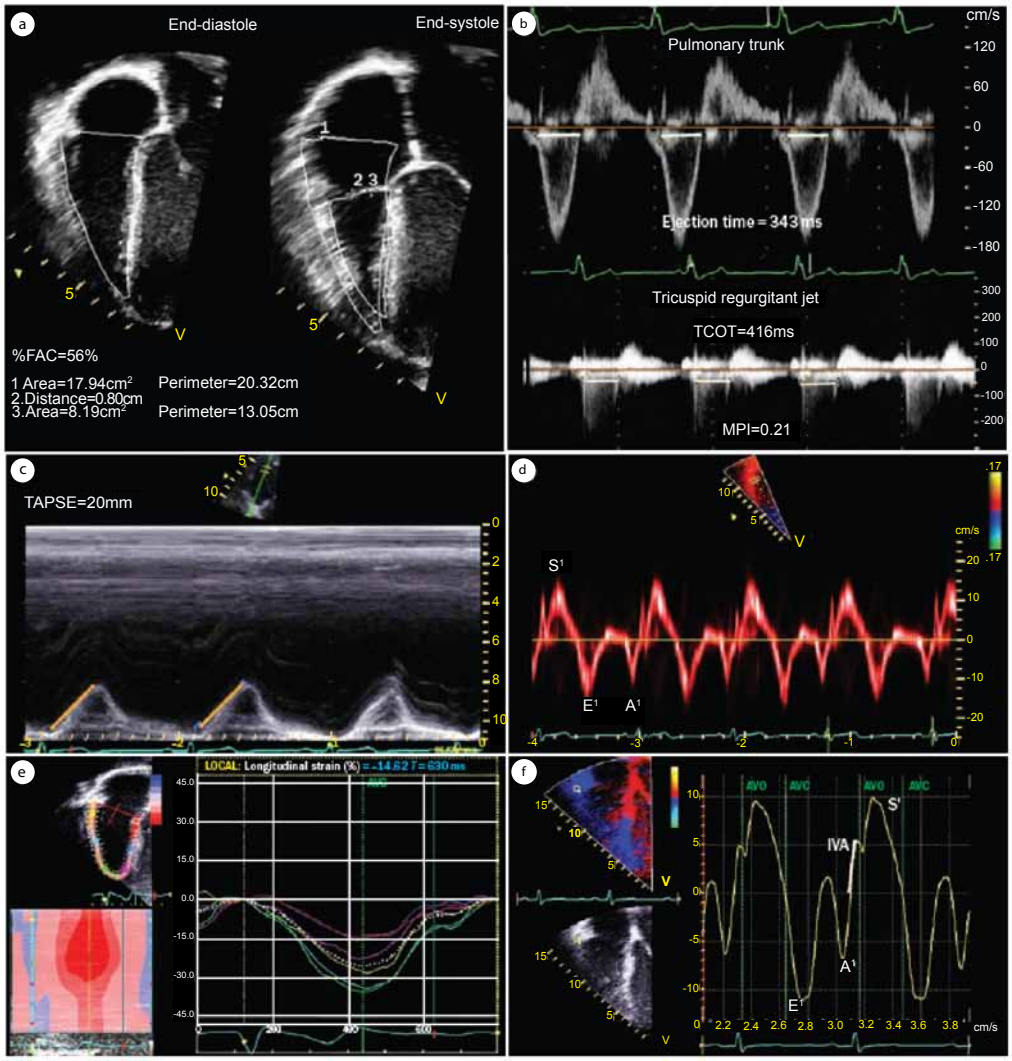

Figure 1: Assessment of right ventricular (RV) function by echocardiography. a) Percentage fractional area change (%FAC), calculated from measures from the apical four-chamber view. b) Myocardial performance index (MPi), calculated by measuring the ejection time on the pulmonary artery tracing and the time between closure and opening of the tricuspid valve on the tricuspid inflow tracing. MPi = Tricuspid valve closure–opening time (TCOT) – ejection time (eT)/eT. MPi was normal after tetralogy of Fallot repair in this patient. c) Tricuspid annular systolic plane excursion (TAPSE). An M-mode echocardiogram through the tricuspid annulus is obtained and the excursion of the tricuspid annulus is measured as illustrated. d) Tissue Doppler velocities of the tricuspid annulus. Pulsed tissue Doppler measurements can be used to calculate tissue velocities. e) Longitudinal strain measurements of the right ventricle, made using speckle tracking technology. By convention, systolic longitudinal shortening is represented as a negative value and can be measured in six different segments. The mean values of these segments are used to trace a mean longitudinal strain curve (white dotted line). The value at end-systole is then measured. f) Color tissue Doppler echocardiogram at the lateral tricuspid valve annulus and measurement of isovolumic acceleration (iVA). Aortic valve opening and closure are depicted by green lines for event timing. The timing of these events may be taken as that of pulmonary valve opening and closure. The slope of iVA is shown. Note that iVA occurs within the QRS complex and peaks before pulmonary valve opening in the isovolumic period. Abbreviations: A', late diastolic tissue velocity; AVC, aortic valve closure; AVO, aortic valve opening; e', early-diastolic tissue velocity; S', systolic tissue velocity. Copyright from Mertens L, Friedberg MK, Nat Rev Cardiol 2010, (doi:10.1038/nrccardio.2010.118) with permission from the publisher, Macmillan Publishers Limited, Copyright approval from Nature Publishing Group.

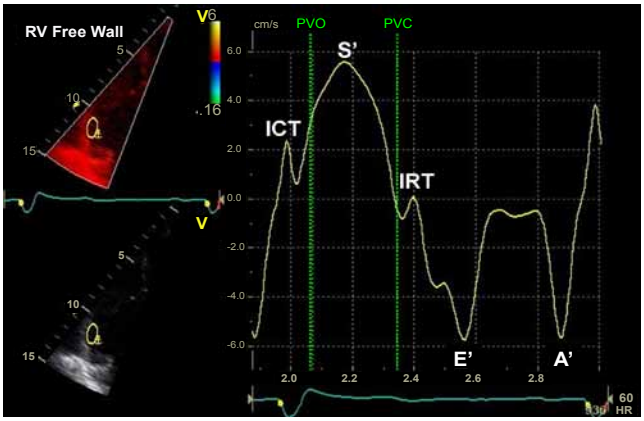

Figure 2: Color DTI waveforms obtained from the RV free wall describing the various phases in ventricular systole and diastole. There are 5 discrete waveforms occurring within the cardiac cycle, as seen on the Doppler display: (1) isovolumic contraction time (ICT) velocity, (2) systolic (S0) velocity, (3) isovolumic relaxation time (IRT) velocity, (4) early diastolic velocity (E0), and (5) late diastolic velocity (A0). Dotted vertical lines represent PV opening (PVO) and PV closure (PVC). Copyright from Horton et al. (J Am Soc Echocardiogr 2009; 22: 776-792) with permission from the publisher, Copyright 2009, the Journal of the American Society of Echocardiography.

Tissue Doppler velocities

In the 1990s, tissue Doppler imaging was recognized as a potentially clinically useful technique for the assessment of global and regional myocardial systolic and diastolic function [5]. As the myocardium moves during the contractile cycle, velocities within the myocardium can be recorded using Doppler technology [5]. By measuring tissue Doppler velocities in different areas within the myocardium, regional myocardial function can be assessed. In patients with normal sinus rhythm, the following waveforms can be seen: the isovolumic contraction (ICT) waveform occurs in early systole; the systolic (S) peak waveform occurs during ventricular mechanical systole and is always displayed above the zero baseline; the isovolumic relaxation (IRT) waveform occurs in early diastole (end of the T wave on electrocardiography); the early diastolic (E) waveform occurs during peak ventricular relaxation (after IRT); and the peak late diastolic (A) waveform represents atrial contraction (Figure 2).

Normal paediatric tissue Doppler imaging (TDI) data has been published [6]. It was shown that tissue velocities vary with age and heart rate. Eidem et al. showed that pulsed-wave TD velocities correlate with cardiac growth variables, i.e., especially LV end-diastolic dimension (LVEDD) and LV mass [6], indicating that tissue velocities are not independent of geometry. The latter has important implications in children with congenital heart disease who have great variability in RV and LV size, mass and geometry. Apart from the influence of geometry, changes in loading conditions also affect TDI velocity measurements: Clinical studies investigated the use of regional myocardial velocities in various adult conditions, such as ischemic heart disease, aortic regurgitation, and hypertrophic cardiomyopathy [7]. In an adult population with aortic stenosis, the degree of reduction in longitudinal systolic LV TDI velocities was shown to be related to the degree of fibrosis in the LV and parameters of longitudinal systolic function were also predictive of outcome after aortic valve replacement [8]. Kiraly et al. [9] showed in children with aortic valve stenosis, peak systolic and early diastolic wall velocities in the four-chamber view were significantly reduced.

As CHD frequently affects the RV, data on right ventricular TDI velocities have been published in several conditions. In the normal (non-hypertrophied) RV, there is predominantly longitudinal orientation of the RV myofibres, making quantification of longitudinal TDI velocities especially important when assessing both systolic and diastolic RV function. Good correlations between systolic velocities and RVEF were found in an adult population that included patients with congenital heart disease [10]. Eyskens et al. [11] showed elevated RV systolic velocities in patients with ASDs and dilated RVs before percutaneous closure of the defect, which normalized within 24 hours after closure. Quantitative assessment of RV performance after repair of tetralogy of Fallot (TOF) has also been investigated. TDI velocities were found to be decreased in TOF patients after surgical repair [12]. All TOF patients had normal LV myocardial velocities in this study while 48 patients (24 patients <18 and 24 >18 years old) had reversed myocardial velocities in diastole in the RV free wall [12].

The use of TDI velocities in a functionally univentricular heart has also been studied. Frommelt et al. [13] used these measurements for the evaluation of 17 patients with hypoplastic left heart syndrome, and showed a non-significant trend towards a decrease in systolic and diastolic tissue velocities from the neonatal period until after second stage palliation, with no difference regarding the type of initial palliation. Mechanical dyssynchrony, as assessed by TDI for example is often present in patients with cardiomyopathy but unrelated to electrical dyssynchrony, and correlates with the severity of LV dysfunction [14,15]. Such mechanical dyssynchrony probably reflects regional differences in myocardial dysfunction. Mechanical dyssynchrony evaluated by TDI was analysed in only 64% of patients in a European multicenter study evaluating the current practice and results of cardiac resynchronization therapy in pediatric CHD [16].

Applications of TDI for RV function analysis in pediatrics have also been investigated. In healthy neonates born at or near term, the longitudinal systolic tricuspid annular velocity was only 1.2 times that of the mitral annular velocity [17]. This ratio of TV/MV excursion velocity differs from adults in whom tricuspid annular velocity far exceeds mitral annular velocity; it is speculated that this discrepancy may be the result of the increased afterload faced by the neonatal vs. the adult RV.

Color TDI was introduced as an alternative technique for measuring tissue velocities. In contrast to pulse wave (PW) Doppler that measures peak velocities, color TDI uses autocorrelation techniques in order to measure regional mean velocities. An advantage of colour TDI vs. PW TDI is that tissue velocities can be recorded simultaneously in different myocardial segments during the same cardiac cycle. Kukulski et al. [18] demonstrated that TDI is feasible for the assessment of RV function by using color TDI to measure regional velocities at the TV annular, basal, mid, and apical regions of the RV free wall in 32 healthy subjects. The authors found significant variability in RV systolic velocities in all myocardial regions among healthy subjects. RV velocities were higher than those recorded in corresponding LV segments. Measurement of longitudinal RV function by TDI is discussed further below in a separate section.

Advantages of TDI in CHD are: (1) the technology can be applied to any chamber morphology, and (2) variables are not based on assumption of chamber geometry. The limitations of PW TDI and color Doppler TDI are mainly related to the variability of the measured velocities with different loading conditions (which also applies to conventional ultrasound measurements), assessment of myocardial motion in a single dimension, and the dependency on

the angle of interrogation. The latter is often more problematic when assessing the RV free wall than the septal or LV free wall. Movement of the entire heart within the chest (translation) during the cardiac cycle and tethering effects between myocardial segments also affect measurements of TDI velocities.

Myocardial performance index (Tei Index)

The myocardial performance index (Tei index) evaluates global ventricular function by measuring the ratio of isovolumic time intervals to ventricular ejection [19]. The longer the isovolumic phases, the higher the Tei index, and the worse the ventricular performance. While the Tei index was initially developed for the assessment of global LV function, Eidem et al. found the Tei index useful in evaluating RV function in patients with CHD [20]. In this study, patients with large atrial septal defects represented the clinical setting of increased RV preload, whereas patients with isolated pulmonary valve stenosis represented increased RV afterload. Patients with congenitally corrected transposition of the great arteries with severe left atrioventricular valve regurgitation represented a combined increase in RV preload and afterload. No significant change in the RV Tei index was seen in any postoperative patient group despite relief of RV volume or pressure overload [20]. The authors suggest that the Tei index is relatively independent of changes in preload or afterload in the clinical setting [20], although chronic adaptation versus acute changes need to be considered.

In the early neonatal period, the RV and LV Tei index as assessed using pulsed Doppler echocardiography were found to inversely correlate with RV output and EF, respectively, while the LV Tei index was found to correlate inversely with LV output and LVEF in the early neonatal period as assessed by PW-Doppler [21]. In addition, both RV and LV Tei index were shown to be significantly impaired in asphyxiated neonates [22]. The Tei index has also been reported to predict the outcome in children with heart failure [23]. Tissue velocity tracings have also been used to calculate Tei index, with significant correlations with PW Doppler measurements [24]. At the lateral and septal site the LV Tei index measured by TDI correlated well with conventional Tei index, both in healthy subjects and in patients with dilated Cardiomyopathy. The highest correlation was observed in TDI Tei index mean values (r = 0.94) in healthy subjects in this study [24]. The use of TDI is also useful for the RV, allowing simultaneous measurement of systolic and diastolic velocities to reflect systolic and diastolic function. The RV Tei index has been assessed in 15 patients after repair of TOF and other forms of CHD [25]. In this study the Tei index obtained by pulsed Doppler method in TOF patients did not differ from that in normal children (0.30 ± 0. 12 vs. 0.32 ± 0.07). The RV Tei index correlated well with pulmonary artery pressure [26] and has been used to identify early RV dysfunction in CHD [20]. Roberson et al. [27] investigated the RV Tei index in children and adolescents. The RV Tei index was calculated in this study by both TDI and PW-Doppler in 308 children. RV Tei index normal value as measured by TDI was 0.37 ± 0.05, and the RV Tei index normal value as measured by PW-Doppler was 0.34 ± 0.06 [27]. Cheung et al. [28] showed that the Tei index is affected significantly by acute changes in loading conditions and was unable to consistently detect acute changes in LV contractile function by calculating the Tei index [28], making its interpretation difficult in the clinical setting. The TDI-Tei index has also been used to assess RV function in patients with pulmonary regurgitation (PR) after TOF repair, and was significantly higher (=impaired) in TOF patients compared with controls, while there was no difference in conventional Tei index between TOF patients and control subjects [25]. In postoperative TOF patients, others have reported a good correlation of the Tei index with RVEF measured by cardiac MRI [29]. The Tei index is a combined ventricular-vascular index that is fairly independent of ventricular geometry.

Limitations of the Tei index include the combination of systolic and diastolic time intervals in a single index which does not allow distinction between systolic and diastolic dysfunction (when the Tei index is abnormal, an appropriate interpretation is "abnormal systolic or diastolic function"). An additional limitation of the RV (vs. LV) Tei index (of blood flow) is that the Doppler beam cannot be aligned in a way that it runs through the RV inflow and RV outflow, which is possible for the mitral inflow and LVOT. Therefore, for the RV Tei index two traces need to be recorded at identical heart rates, which may be impractical in the clinical setting. Caution is warranted when interpreting RV Tei indices obtained at even slightly different heart rates.

Myocardial acceleration during isovolumic contraction (IVA)

Isovolumic acceleration resembles myocardial motion during the isovolumetric contraction period. During this time period there is myocardial motion, related to the shape change from a more spherical ventricle to an ellipsoid. The rate of myocardial acceleration during the isovolumic period has been described to correlate with intrinsic myocardial contractility and is thought to be relatively independent of loading conditions [30]. IVA is determined by tissue Doppler and can be used to assess contractile reserve during regular exercise stress testing [31] and stress echocardiography [32]. IVA has also been validated as a sensitive non-invasive index of LV and RV contractility [33]. Normal adult values of IVA measured in the basal segment of the RV free wall are >1.1 m/s^2. An example is shown in Figure 3. The heart-rate sensitivity of IVA has been used to assess contractile reserve by studying the force-frequency relationship during pacing, dobutamine stress echocardiography or exercise [32,34]. In paediatric patients, LV IVA has been used after heart transplantation, where it was suggested to

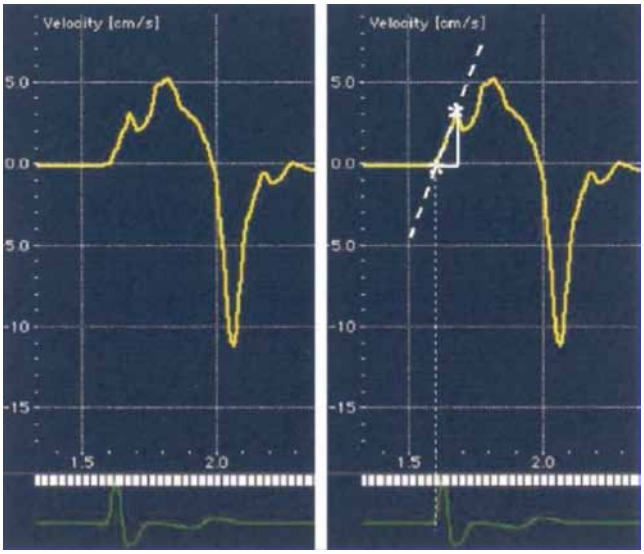

Figure 3: Tissue Doppler echocardiography spectral curve at the level of the tricuspid annulus. The isovolumic myocardial acceleration is calculated as the difference between baseline and peak velocity (stars) during isovolumic contraction divided by their time interval. Reproduced from Vogel et al. [30] with permission from the publisher; Copyright © 2004, the American College of Cardiology Foundation.

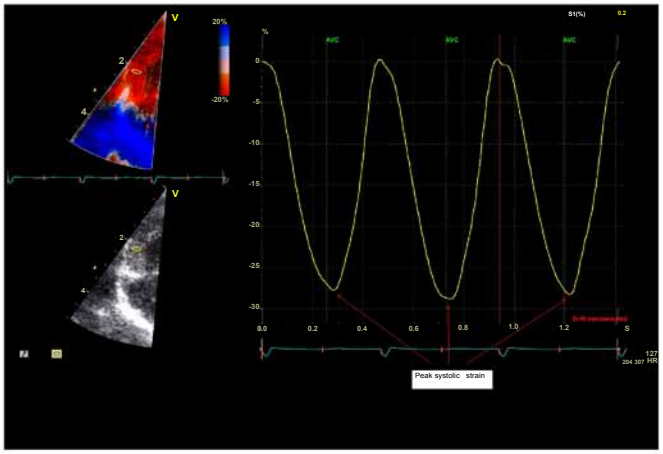

Figure 4: Analysis of strain by tissue Doppler from the mid segment of the right free wall obtained from the apical 4-chamber view in a healthy term neonate. Upper left Figure: Strain by tissue Doppler image. Lower left Figure: Grey-scale image. Right Figure: Strain curve for three consecutive heart beats. Red arrows mark the peak systolic strain values.

be a useful additional non-invasive indicator of allograft rejection [35]. Vogel et al. [30] used tricuspid annulus IVA to assess the systemic RV in patients who had undergone an atrial switch procedure for d-TGA. The tricuspid IVA in this population was lower than the corresponding LV IVA. In patients with repaired TOF, RV IVA was also shown to be decreased and inversely related to the degree of PR, suggesting reduced contractile RV function in these patients. RV systolic dysfunction in patients with mitral stenosis could also be detected early by abnormal IVA [34]. Cheung et al. described a preserved systolic contractile reserve in children with single ventricle physiology after Fontan operation [36].

Taken together, IVA is a relatively load-independent measure of RV function.

Limitation of IVA includes its dependency on heart rate and according to our experience - a high interobserver variability.

Deformation imaging

Wall motion abnormalities are relatively common in patients with CHD. Strain and strain rate seem to be useful in detecting such motion abnormalities. Regional deformation (strain) and strain-rate can be calculated non-invasively in both the LV and RV, providing information on regional myocardial dysfunction in a variety of clinical settings. Myocardial velocities and displacement are influenced by global cardiac translational motion and by motion in adjacent myocardial segments (myocardial tethering) which limits their use in the assessment of regional myocardial function. This limitation can be overcome by using regional myocardial deformation or strain imaging (Figure 4).

Myocardial strain and strain rate are measures of deformation within segments of the myocardium and provide additional information on myocardial mechanical function. Strain is expressed as the percentage change in length from the original length. Strain rate is the rate of deformation (per second). Assessment of values from several segments can be done simultaneously. Strain imaging can quantify RV function in patients with CHD [37] and detect subclinical myocardial dysfunction both in patients receiving anthracyclines [38] and in young patients with muscular dystrophy [39]. Weidemann et al. first published deformation values in healthy children [40]. Deformation imaging has recently also been performed in healthy [41-43] and in asphyxiated neonates [44].

Two different technologies are currently available for studying regional myocardial deformation. The first technique is based on TDI and calculation of myocardial velocity gradients. The second method is based on tracking speckles on the grey-scale images from frame to frame throughout the cardiac cycle, and calculating the displacement of the speckles throughout the cardiac cycle ("speckle tracking").

Tissue Doppler-derived deformation imaging: TD-derived deformation imaging is based on assessment of differences in tissue velocities within myocardial segments and reflects either lengthening or shortening of the segment in the longitudinal, radial or circumferential dimension. Strain rate is calculated as the velocity difference between two or more points within the myocardial segment divided by the distance between them, assessing the velocity gradient within the segment. Such velocity gradients actually quantify the instant regional deformation within the segment, expressed as the strain rate. The strain value is assessed by temporal integration of the strain rate values. The temporal resolution is high, and higher than that of two-dimensional speckle tracking techniques and MRI. The disadvantages of TDI-derived deformation imaging are its angle-dependency and the required post - processing [45]. Measurements are prone to artifact from poor image quality and the reproducibility can be low. Despite these limitations, radial strain evaluation in the LV posterior wall has been suggested as a reproducible technique that performs better than speckle-tracking techniques [45] where reproducibility for radial strain was poor. Longitudinal strain measurements in the interventricular septum, and LV and RV lateral walls have been used to quantify regional and global myocardial function. LV ejection fraction is generally preserved in patients with hypertrophic cardiomyopathy (HCM), but deformation imaging has demonstrated significant regional differences in systolic deformation. Peak systolic strain was shown to be reduced significantly in the more hypertrophic regions of HCM patients [46,47]. In young patients with Duchenne muscular dystrophy, deformation analysis showed a significant decrease in radial and longitudinal peak systolic strain and strain rate in the LV inferolateral and anterolateral walls in patients with normal EF [48]. In patients studied during follow-up after anthracycline exposure, a decrease in deformation variables was observed, despite normal EF and fractional shortening [49]. Eyskens et al. [50] demonstrated that TOF patients had decreased peak systolic strain and strain rate values in the basal, mid and apical segments of the RV free wall and interventricular septum which was related to the degree of pulmonary regurgitation. Reduced regional peak systolic strain and strain rate values in the apical segments of the RV free wall were also found in CHD patients with a systemic RV [37]. Bos et al. described reduced longitudinal RV deformation in patients with congenitally corrected transposition of the great arteries [51].

Two-dimensional-based deformation imaging - speckle tracking: Speckle tracking is based on grey-scale images and is relatively easy to perform. In contrast to TDI derived parameters, speckle tracking is an angle independent technique as the movement of speckles can be followed in any direction within the 2d grey scale image. As the method is based on recognition of speckles between frames, there are upper and lower limits for the frame rate. The frame rate has to be high enough so that speckles are recognizable between frames. Speckle tracking is influenced by frame rate and is limited by movement out of the plane. As a high frame rate is obtained mainly by reducing the lateral beam

density, a high frame rate could impair the tracing of speckles due to low lateral spatial resolution. The temporal resolution is low compared to TDI, which might be an issue especially in smaller children with higher heart rates. The low frame rate probably has a higher influence on the strain rate than on the strain measurements. Strain rate by speckle tracking is not routinely assessed in children. Current two-dimensional longitudinal deformation analysis is largely based on assessment of the AV-valve plane motion. Regional differences might therefore not be detected, but at the same time the global values might be less influenced by local or regional artefacts. Software from different vendors can yield different results [45]. Good correlation between two-dimensional speckle strain and MRI tagging for the LV and RVs has been reported [52,53]. The major clinical applications of speckle-tracking techniques should be the same as for the TDI-derived techniques. As described recently, the major advantage of speckle-tracking technology is the ability to study radial, longitudinal and circumferential deformation as well as the assessment of ventricular rotation and torsion [54]. Kowalski et al. [55] reported decreased deformation in the LV anterior wall after successful repair of aortic coarctation. Laser et al. [56] showed in patients with aortic stenosis and aortic coarctation, LV torsion was increased before and decreased after interventional treatment. Dragulescu suggested that speckle-tracking techniques can be used in children to reliably quantify longitudinal and circumferential strain [57]. Left ventricular torsion seems to be impaired in conditions associated with RV volume load, mostly due to reduced basal rotation. In young adults, acute unloading of the RV after transcatheter closure of a secundum ASD improves LV twist by increasing basal rotation [58]. Cheung et al. showed that RV dilatation has a negative impact on LV circumferential deformation but not longitudinal or radial deformation [59]. Kutty et al. investigated the changes in RV function in patients after TOF repair and surgical pulmonary valve replacement [60]. A significant increase in peak systolic velocities (but not in global longitudinal strain) was seen, and all indices remained significantly lower in TOF patients compared with healthy controls. A recent study evaluated the acute effect of transcatheter pulmonary valve implantation, demonstrating a short-term improvement in RV free wall and septal longitudinal function [61]. However, most studies have not shown intermediate term improvement in RV strain after transcatheter pulmonary valve implantation.

Comparison of TDI and 2D-based deformation imaging: Normal values of Tissue Doppler velocities, strain, and strain rate measurements in pediatric and adult healthy subjects are shown in Table 1. Tissue velocities and strain measurements have been shown to be useful to quantify global and regional RV function in adult pulmonary arterial hypertension (PAH) patients. The more severe the PAH, the lower the end-systolic longitudinal strain in the RV free wall [62,63], demonstrating a dependence of systolic RV longitudinal strain measurement on RV afterload [64,65]. In a comparison of TDI and 2D speckle tracking, comparable values were found for speckle tracking and TDI in both normal and dysfunctional segments and in radial measurements, but 2D speckle tracking was suggested to be more reliable than TDI [66]. TDI is not possible when the ventricular wall is not optimally aligned to the beam, or in the presence of a stationary artefact. A disadvantage of two-dimensional speckle tracking lies in its relative low temporal resolution that hinders tracking in the presence of high heart rates [67]. Further, at high heart rates the low temporal resolution can lead to undersampling of the true peak values, as these might occur between the frames recorded. Post processing time was shown to be significantly shorter with speckle tracking compared to TDI analysis [68]. Teske et al. reported that the quantification of regional RV function using either 2D speckle tracking or TDI is feasible and reproducible [53,69]. 2D Strain and strain rate might be relatively

	Neonates/ infants	Children	Adults	Intra-observer variability	Inter-observer variability	References
TDI						Kukulski (18) Eidem (125)
S' (basal)	10.2 ± 5.5 PTDI	12.8 (10.7-16.5) 16.1 ±4.7 PTDI	15.2 ± 2.8 PTDI	6.17 (COV)	8.82 (COV)	
E'(basal)	13.8 ± 8.2 PTDI	-16.2 (-12.6 to -21.1) PTDI	14.5 ± 3.5 PTDI	2.2% - 3.4% (mean % difference)	1.6% - 2.0% (mean % difference)	
A'(basal)	9.8 ± 2.4 PTDI	-8.6 (-5.5 to -12.1) PTDI	16.2 ± 3.1 PTDI			
Strain				12.9 (mean % diff)	14.4 (mean % diff)	Weidemann (40) Pena (42)
Basal	-28.38 ± .90 CTDI	–36 ± 11 CTDI	19±6	NA	NA	
Mid	-33.20 ± .34 CTDI	–45 ± 13 CTDI	27±6	NA	NA	
Apical	-31.95 ± 5.06 CTDI	–34 ± 11 CTDI	32±6	NA	NA	
Strain rate				11.8 (mean % difference)	13.6 (mean % difference)	Weidemann (40) Pena (42)
Basal	-1.93 ± 0.52 CTDI	–2.4 ± 0.6 CTDI	1.5±0.41	NA	NA	
Mid	-1.91 ± 0.45 CTDI	–2.8 ± 0.7 CTDI	1.72±0.27	NA	NA	
Apical	-1.81± 0.40 CTDI	–2.5 ± 0.6 CTDI	2.04±0.41	NA	NA	

Table 1: Tissue Doppler velocities, strain and strain rate- normal RV value. The values in the table are shown as follows. For each age group the standard deviation (s) was taken to construct ranges of the mean ± 2s. Abbreviations: A`, peak late diastolic velocity, COV, coefficient of variation; CTDI, color tissue Doppler imaging, E`, peak early-diastolic velocity; NA, not available; PTDI, pulsed tissue Doppler imaging; S`, peak systolic velocity. Copyright from Mertens L, Friedberg MK, Nat. Rev. Cardiol 2010, (doi:10.1038/nrccardio.2010.118) with permission from the publisher, Macmillan Publishers Limited, Copyright © approval from Nature Publishing Group.

independent of loading conditions and preferred over tissue velocities as they are not influenced by passive motion of the myocardium when the heart moves within the chest. The software and techniques used for assessment of strain and strain rate continues to develop. The future ease of using 2D-based deformation imaging techniques with limited post-processing times will probably results in a more routine application of this technique, but at present the different solutions offered by the competitive software vendors remains a major challenge, and the need for an industry standard for these measurements is needed [45].

Tissue tracking of cardiac magnetic resonance images (CMR) is a novel method with only little published research on this topic [70-73]. Niemann et al. introduced speckle-tracking by velocity vector imaging applied to CMR imaging in normal hearts [70]. In patients with a single ventricle a decrease in apical rotation and circumferential strain compared to controls was found [71]. The authors concluded that speckle-tracking applied to CMR imaging sequences was able to detect reduced strain and rotational motion in patients with single ventricle. Ortega et al. [72] investigated the impact of LV dyssynchrony on clinical outcomes of TOF patients. Using tissue tracking applied to CMR images they were able to identify indexes of LV synchrony associated with death and ventricular tachycardia in patients with repaired TOF. For a detailed description of strain analysis of CMR sequences we refer to Truong et al. [71].

Three-dimensional echocardiography: Three-dimensional (3D) echocardiographic rendering of cardiac structures of patients with CHD attracted attention during recent years with the development of high-frequency matrix-array paediatric probes with improved image resolution [74]. Full volumetric datasets of the beating heart can be obtained and then cropped to analyze cardiac anatomy. More recently, single beat acquisition of the entire cardiac volume has become commercially available. The latter modality addresses "stitching" artefacts created by the joining of 4-7 sub-volumes to capture the entire cardiac volume, but comes at the expense of reduced frame rates. This issue may be important because matrix-array 3D imaging has lower frame rates than 2D imaging, a relevant consideration in children with high heart rates. In terms of functional imaging, volumetric assessment of the LV and especially the RV is of interest to pediatric cardiologists. Accurate measurement of RV volumes is also important in CHD such as postoperative TOF, where RV end-diastolic volume index is an important variable in the decision for timing of pulmonary valve replacement. There are currently several approaches to assess RV volumes using 3D echo. One approach uses matrix array probes to acquire a full-volume. The ventricle is then segmented into cross sectional planes and the method of discs is used to calculate the ventricular volume at end systole and end-diastole [75,76]. This technique is comparable to volume analysis by MRI. The most common method of assessing RV volume uses semi-automated border detection from a matrix-array full-volume acquisition to reconstruct RV volumes. This technique has been described to be feasible in patients with CHD [77,78], although it may be less accurate and reproducible in CHD than in structurally normal hearts [79]. A third approach uses 'knowledge-based reconstruction' to determine 3D RV volumes from multiple 2D images. The position of the transducer in space is determined using a magnetic tracking system. The RV endocardium and points of reference are marked on the 2D images to encompass the RV in different regions. Data are transferred over the internet to a server, where analysis is performed using a central database of hearts with the lesion of interest (e.g. tetralogy of Fallot). The algorithm then reconstructs the RV volume using both the specific points marked and the databank [78]. With the newer generation of echocardiography machines, enddiastolic volume calculations of 3D datasets correlate well with MRI [80-82]. However, 3D echocardiography is very dependent on adequate acoustic windows. Khoo et al. [83] focussed on determination of RV volumes in adolescents and young adults with CHD. Using different quantification techniques, 3D measurements were only feasible in about 50% of all patients [83], due to inadequate image quality. Likewise, although the authors only used "good" imaging data sets for their analysis, they found about 20 percent lower RV volume values when compared to MRI measurements [83]. A similar underestimation of the RV volume when compared to MRI measurements was reported from a different group that found underestimation of RV volumes by 3D echocardiography mainly in severely dilated RVs [84]. Higher feasibility of 3D echo for RV assessment in patients with CHD has been demonstrated by van der Zwaan et al. [82,85], also with underestimation of RV volumes by 3D echocardiography versus MRI. In patients with PAH, good correlation was found in the measurements of RVEF (r = 0.66) and RVEDV (r= 0.74) determined by either 3D echocardiography or MRI measurements [86]. The use of 3D mode has been validated for the measurement of RV volumes, and EF, which correlated well with those variables determined by CMR imaging in adult and pediatric populations [87,88]. Moreover, Kjaergaard et al. [89] reported the use of 3D echocardiography for the evaluation of RV cardiomyopathy. Normal values for right ventricular size and function in adults have been published [90]. 3D echocardiography outperformed 2D echocardiography in the assessment of RV volumes, and compared favourably with cardiac MRI (r = 0.71-0.97) [91]. Further clinical validation is needed in larger cohorts for the assessment of right ventricular volumes in children with CHD. Validation of 3D echocardiographic assessment of LV volumes and LVEF in children with complex congenital heart disease including a small LV has been performed [75]. Soriano et al. have assessed volume and ejection fraction in pediatric patients with a functional single ventricle using 3D echocardiography and CMRI [76]. The 3D echocardiographic end-diastolic volumes correlated well with CMRI (r = 0.96) but were smaller than CMRI (by 9%). EF by 3D echocardiography was lower than EF by CMRI (by 11%). There was no significant difference between end-systolic volumes and mass [76].

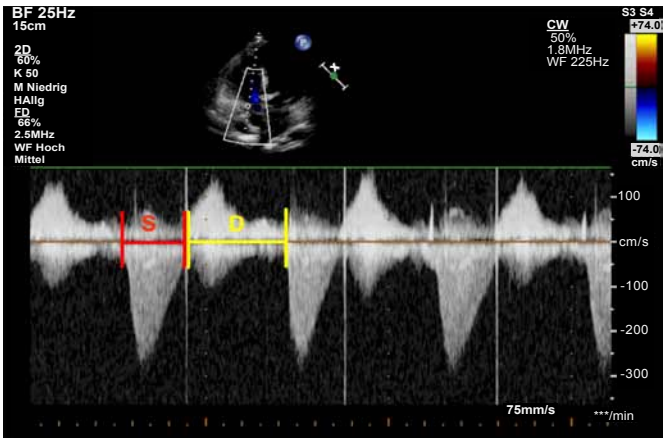

Figure 5: Apical 4-chamber view. Doppler-derived tricuspidal regurgitation time (TR) interval ratio of systolic (S) duration to diastolic (D) duration (S/D) The ratio of S/D duration was calculated by dividing the duration of the TR spectral Doppler flow pattern by the time interval of the cardiac cycle that did not include TR. Systolic and diastolic duration using TR duration was measured by CW-Doppler from the apical 4-chamber view to calculate the S/D ratio. The red lines show the systolic duration, the yellow lines show the diastolic duration.

Three-dimensional echocardiography has also been studied for the evaluation of anatomical aspects of various CHD lesions including atrial and ventricular septal defects, atrioventricular septal defect, congenital mitral stenosis, RV and pulmonary valve outflow tract pathology, aortic valve stenosis and Ebstein's anomaly [92-101]. Cui et al. [102] used the 3D echocardiography to define normal values for LV real-time quantitative 3D echocardiographic dyssynchrony indices (DI). In 102 normal children aged 1 day to 19 years LV 3D echocardiographic DI were obtained. The authors found that 3D echocardiographic DI analysis is feasible and reproducible in most children. Anatomical evaluation by 3D echocardiography may improve delineation of morphology when 2D imaging is inadequate, and provides the surgeon with a realistic view of the anatomy [103]. Anatomical evaluation by 3D echo will not be covered further in this review.

Systolic to diastolic deviation ratio: Recently Friedberg et al. [104] described the Doppler-derived mitral regurgitation time interval ratio of systolic (S) duration to diastolic (D) duration (S/D). The S/D duration ratio was found to be abnormally increased in children with dilated and restrictive cardiomyopathy [104,105]. The S/D ratio was calculated by dividing the duration of the mitral regurgitation (MR) spectral Doppler flow pattern by the time interval of the cardiac cycle that did not include MR [104]. Patel et al. [106] described their clinical

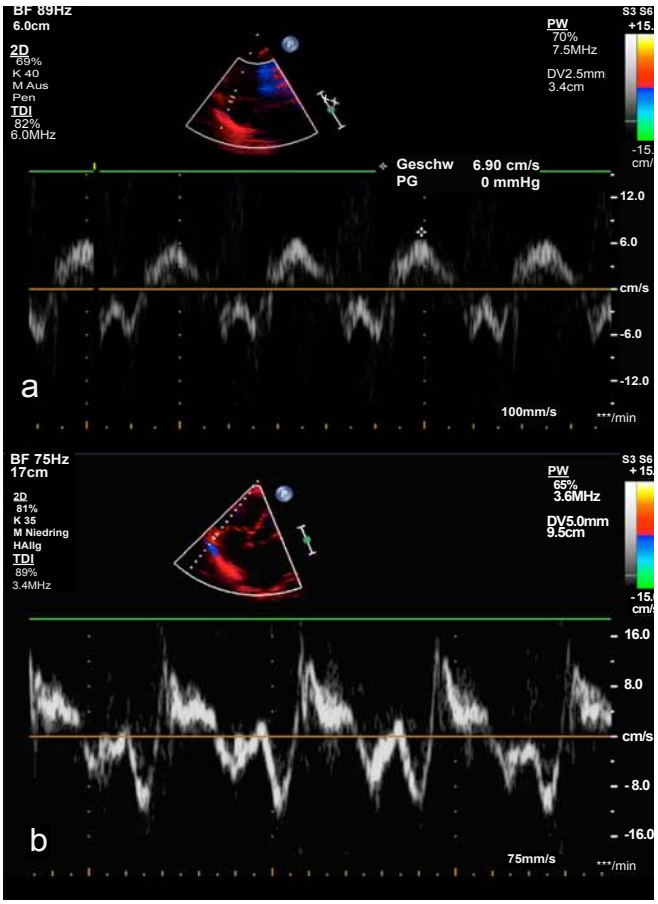

Figure 6: Apical 4-chamber view. The white broken line indicate M-Mode cursor placement at the tricuspid lateral annulus. Representative image of the tricuspid annular peak systolic velocity (TAPSV) in a neonate (Figure 1a), and in a 15 year old adolescent (Figure 1b), respectively, with normal right and left ventricular function.

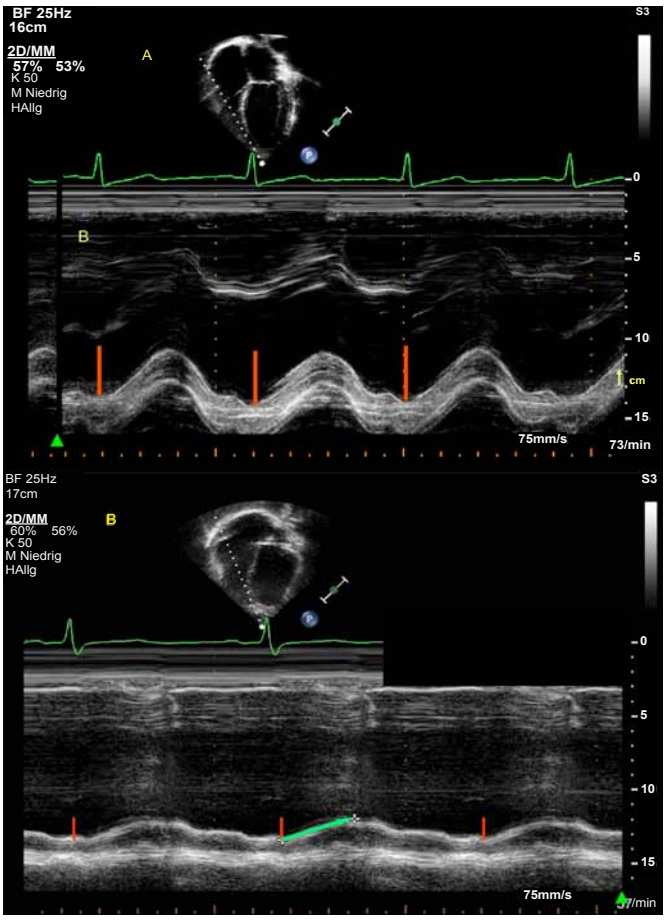

Figure 7: Apical 4-chamber view. (A) The white broken line indicate M-Mode cursor placement at the tricuspid lateral annulus. Representative M-Mode image of the tricuspid annular plane systolic excursion (TAPSE) in a patient with normal right and left ventricular function. The absolute longitudinal displacement measure is shown as the red line. The yellow arrow marks the upper and lower measure point of one centimeter (cm). (B) Representative M-Mode image of the tricuspid annular plane systolic excursion (TAPSE) in a 17 year old patient with TOF and a decreased TAPSE. The absolute longitudinal displacement measure is shown as the red line. The green arrow shows the decreased TAPSE value and flat course of the excursion.

impression that Tei index and S/D ratio occasionally lack sensitivity and have a low negative predictive value due to a significant false-negative rate. Friedberg et al. [107] investigated the S/D duration ratio in children with HLHS as a novel index of global RV function. They measured systolic and diastolic duration using tricuspid regurgitation (TR) duration by CW Doppler to calculate the S/D ratio in children with HLHS. Recently, changes in the S/D ratio measured by TDI in HLHS were attributed predominantly to changes in heart rate [108]. Indeed heart rate has been shown to be a major determinant of D and S duration; at resting heart rates, systole (S) constitutes about 40% of the cardiac cycle in healthy children [107]. An example is shown in Figure 5. In patients with PAH, RV contraction is prolonged, although RV ejection time is shortened, so that S/D duration was proposed as an indicator of PAH severity [109]. Alkon et al. [110] found that children with significant PAH have a marked decrease in diastolic duration and increase of the S/D duration ratio when their heart rate increases compared to matched control subjects. Alkon et al. [110] found that an increased S/D duration ratio > 1.4 inversely correlates with survival in

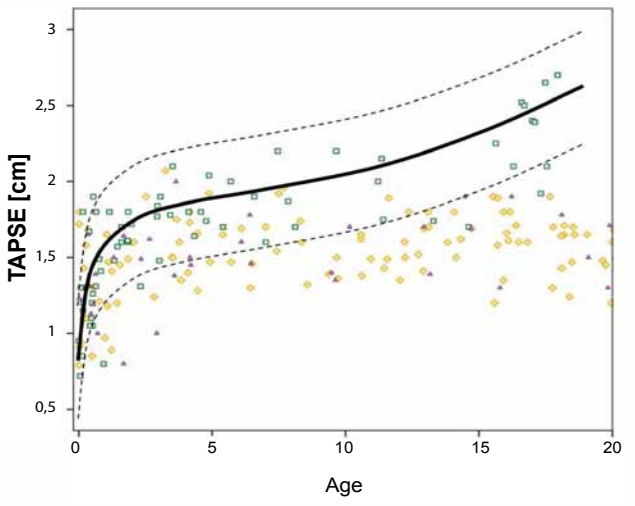

Figure 8: Course of tricuspid annular plane systolic excursion (TAPSE) values in patients with pulmonary artery hypertension (PAH), pulmonary stenosis (PS), and tetralogy of Fallot (TOF) from mean reference values versus increasing time period. The TAPSE value data points for PAH, PS, and TOF patients are given as yellow oblique squares, green squares, and purple triangles, respectively. The interpolated mean values of control group are given as the black thin line. The -2 standard deviation line (-2SD) of the control group measurements is given as a grey dashed line. The difference of mean TAPSE values from mean reference values is expressed centimeter (cm).

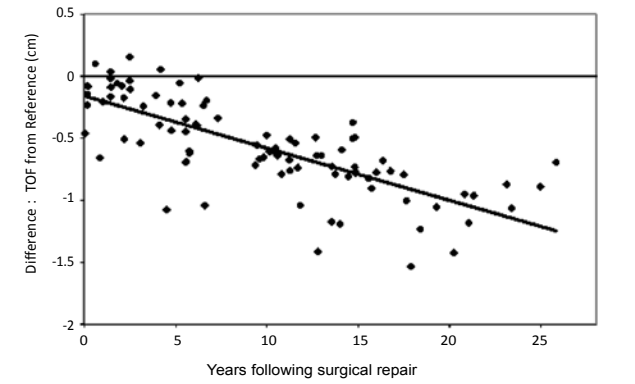

Figure 9: Deviation of tricuspid annular plane systolic excursion (TAPSE) values in tetralogy of Fallot (TOF) patients from reference values versus years following surgical repair. The TAPSE value data points are given as black dots. Shown is the absolute deviation of the measured TAPSE values of TOF patients compared to TAPSE reference values. The difference of TAPSE values is expressed in centimetre (cm). The black solid line is an interpolation for a linear trend for the TOF patients.

children with PAH [110]. The authors concluded that in children with PAH, an increased S/D ratio is temporally associated with worse RV function, hemodynamics, exercise capability, and survival.

Limitations of S/D duration ratio: The measurement of S/D duration ratio requires the presence of clearly defined onset and end of MR/TR on spectral Doppler tracings. The S/D duration ratio is influenced by heart rate and by loading conditions.

Measurement of longitudinal RV function: The RV differs from the LV in its physiology with the LV output being less sensitive to afterload changes than the RV [2], and this might explain that PAH is less tolerated compared to systemic arterial hypertension [2]. Echocardiographic assessment of RV function is known to be difficult in both children and adults. The anterior position of the RV in the chest limits the echocardiographic visualization of the RV. Moreover, the RV has a complex geometry, with a triangular shape in the sagital and a more crescent shape in the coronal plane. Furthermore the RV inflow and outflow tracts are difficult to image simultaneously with 2-dimensional echocardiographic methods. In a normal RV, most of the myocytes are orientated longitudinally, which results in a different contraction pattern when compared to the LV [111]. Indices for assessment of longitudinal RV function have been published, including tricuspid annular plane systolic excursion (TAPSE) [112] (Table 2), and tricuspid annular peak systolic velocity (TAPSV) [113] (Figures 6,7). Measurement of myocardial velocities by TDI is a promising approach for quantitative assessment of longitudinal systolic ventricular performance [114]. TDI indicates systolic ventricular performance by measuring velocities directly within the myocardium. By employing pulsed wave (PW)-TDI to the tricuspid annulus, it is possible to measure its peak systolic velocity [115]. The TAPSV, measured by PW-TDI, has been suggested as a quantitative parameter of RV systolic function in adults [116] and in children [117].

The TAPSE is an indicator of ventricular contractile function that correlates well with RVEF in adults [118], and has been investigated as an index of systolic RV function in pediatric patients with TOF and ASD [119,120]. Reference values of TAPSE measurements in adults and across the full pediatric age range are available [121,122], (Table 2). In recently published recommendations for the performance of a pediatric echocardiogram the value of TAPSE measurement is discussed in detail and recommended as an additional tool for the investigation of longitudinal RV function [123]. TAPSE has been shown to be too insensitive to detect minor RV volume changes in pediatric patients with an unrepaired isolated atrial septal defect but did reflect reduced RV systolic function in postoperative pediatric patients with TOF [119]. Studies of PW-TDI measurements of the tricuspid annular velocity in children have been published [117, 124,125], and report conflicting data regarding the impact of age on TAPSV in pediatric

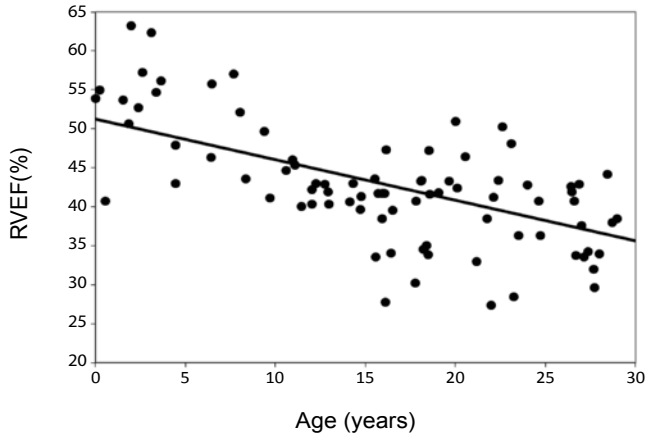

Figure 10: Relationship between age and right ventricular ejection fraction (RVEF) mean values (in %) of TOF patients are given as a typical scatter plot. The tricuspid annular plane systolic excursion (TAPSE) value data points are given as black dots. The black solid line is an interpolation for a linear trend for the TOF patients.

		TAPSE (cm)					BSA (m^2)			
			Bounds for z-score-ranges							Indexed TAPSE Mean/ BSA Mean
Age	n	Mean	±2s (95%)		±3s (99%)		Mean	Min	Max	
0 - 30 days	41	0.91	0.68	1.15	0.56	1.26	0.22	0.14	0.28	4.14
1 - 3 months	45	1.14	0.85	1.42	0.71	1.56	0.29	0.12	0.54	3.93
4 - 6 months	20	1.31	1.01	1.65	0.86	1.77	0.34	0.26	0.41	3.85
7 - 12 months	22	1.44	1.13	1.77	0.97	1.91	0.40	0.31	0.47	3.6
1 years	25	1.55	1.25	1.88	1.10	2.00	0.47	0.3	0.69	3.29
2 years	39	1.65	1.36	1.94	1.22	2.09	0.53	0.4	0.62	3.11
3 years	27	1.74	1.48	2.02	1.35	2.14	0.63	0.52	0.77	2.76
4 years	47	1.82	1.56	2.07	1.43	2.20	0.70	0.6	0.91	2.60
5 years	29	1.87	1.60	2.13	1.47	2.26	0.77	0.63	0.99	2.42
6 years	41	1.90	1.62	2.18	1.48	2.33	0.82	0.46	1.06	2.31
7 years	32	1.94	1.64	2.25	1.49	2.39	0.94	0.75	1.17	2.06
8 years	23	1.97	1.67	2.28	1.52	2.43	0.97	0.79	1.39	2.03
9 years	20	2.01	1.73	2.30	1.58	2.44	1.00	0.8	1.32	2.01
10 years	27	2.05	1.79	2.31	1.65	2.46	1.15	0.82	1.54	1.78
11 years	25	2.10	1.83	2.36	1.69	2.50	1.28	1.06	1.55	1.64
12 years	18	2.14	1.84	2.43	1.68	2.60	1.39	1.08	1.67	1.53
13 years	20	2.20	1.85	2.54	1.68	2.71	1.48	1.03	1.87	1.49
14 years	35	2.26	1.87	2.65	1.68	2.84	1.55	1.11	1.93	1.46
15 years	25	2.33	1.93	2.75	1.74	2.92	1.59	1.32	1.96	1.46
16 years	34	2.39	1.98	2.78	1.78	3.01	1.66	1.3	2.04	1.44
17 years	27	2.45	2.04	2.88	1.83	3.06	1.77	1.43	2.06	1.38
18 years	21	2.47	2.05	2.91	1.84	3.10	1.79	1.34	2.25	1.37

Table 2: Classification table for the TAPSE values. The values in the classification table are shown as follows. For each age group the standard deviation (s) of TAPSE was taken to construct ranges of the mean ± 2s and ± 3s. These ranges represent the expectable normal intervals of deviation for a certainty level of 95% and 99%. Further the mean, the minimum and the maximum of BSA was calculated for the several age groups. An index was calculated of the TAPSE mean for age divided by the BSA mean for each age group. Abbreviations: TAPSE, tricuspid annular plane systolic excursion; BSA, body surface area; s, standard deviation. Copyright from Koestenberger et al. (J Am Soc Echocardiogr 2009; 22(6):715-9) with permission from the publisher, Copyright © 2009, the Journal of the American Society of Echocardiography.

patients. This discrepancy may be due to small sample sizes, limited age distribution, or somewhat arbitrary age groups. Focussing on the TDI velocities, Roberson et al. [124] provide normal values of systolic S wave of tricuspid annulus in the pediatric age group. However, this study reports a wide range of normal values from infancy (z-score ± 2: 2 cm/s up to 18 cm/s) to adolescents (z-score ± 2: 7 cm/s up to 22 cm/s). In contrast, adult studies show that a TAPSV below 10.5 cm/s [116] is able to predict impaired RV systolic function. A significant positive correlation between TAPSV and TAPSE has been shown in adults with PAH (r = 0.90) [116].

It has been shown that TAPSE is a reproducible index of RV systolic function in patients with PAH; abnormal TAPSE (below 1.8 cm) had a high specificity for abnormal RV function in adults [126]. For every 1-mm decrease in TAPSE, the unadjusted risk of death increased by 17% for PAH patients [126]. A significant proportion of PAH in childhood is associated with CHD [127]. New echocardiographic techniques have been published with the aim to estimate pulmonary artery pressure [128]. An abnormally low TAPSE was associated with poor prognosis in adults with idiopathic PAH [126]. Adult studies describe the usefulness of TAPSE to diagnose RV systolic dysfunction [129,130]; it has been shown that a TAPSE < 2 cm indicates a RVEF of < 40 % [131]. Recently it has been reported that TAPSE measurement is a more reproducible indicator of RV function when compared to other echocardiographic variables such as the RV fractional area change [126]. TAPSE appears to be a developmentally dependent variable that increases from preterm infants to healthy adolescents [120,132]. In an ongoing investigation in PAH patients, with increasing age TAPSE values become significantly decreased compared to age-matched controls, i.e. the longer the RV is exposed to severe pressure overload and potentially other conditions and environmental factors associated with PAH, [Koestenberger M, unpublished data], as shown in Figure 8. Despite the difficulty in determining the exact onset of PAH in the individual patient, this may point towards an early decline of RV systolic function. After a mean of 6.1 years after surgical correction of TOF, TAPSE values become significantly decreased and abnormal (> 2 SD of age-matched controls), indicating reduced RV systolic function

that is likely due to volume overload caused by significant PR [120] (Figure 9). This observation is in agreement with a study showing RV systolic dysfunction in adult TOF patients [133]. In TOF patients with a decreased TAPSE (z-score < -2 SD), an inverse and significant correlation was found between TAPSE and RVEF measured by MRI in 88 children (r = 0.54) [112] and in adults (r = 0.48) [134] (Figure 10). In the pediatric age group, a significant positive correlation was found in 131 TOF patients between QRS duration and RVEDV index (r = 0.66), and QRS duration significantly increased with time after surgical repair (r = 0.81) [120].

Of note, although TAPSE appears to be a good indicator of global RV function, it does not take into account segmental RV function and contractility.

Future Applications of TTE

The perspective of recently developed or advanced echocardiographic techniques and variables, such as tissue Doppler imaging (TDI), deformation imaging (tissue tracking), myocardial performance index, myocardial acceleration during isovolumic contraction (IVA), S/D duration ratio, 3D echocardiography, and measurements of systolic RV function, depends on further validation and demonstration of clinical utility. There is still a long way to go before relevant clinical decisions can be based on these new echocardiographic measures. In particular, prospective comparative studies, and randomized controlled trials using these variables are desirable. However, the new imaging methodologies already offer new insights into the effects of congenital heart disease on LV, RV and vascular function and mechanics. The assessment of ventricular function by echocardiography is an area that is undergoing intensive research, as the development and implementation of new modalities become available. Cardiac sonographers should become familiar with both traditional and newer techniques such as tissue Doppler imaging, deformation imaging, S/D duration ratio, 3D echocardiography, and measurements of systolic RV function, for more detailed assessments of ventricular performance.

Literature Search

This review article is based on a literature search in the PubMed database. Papers published in English as full-text research articles or review articles were accepted. The key words used were “right ventricular function”, “left ventricular function”, “echocardiographic assessment”, “and imaging”. Since the most recent developments in echocardiography are the focus of his review article, predominantly papers published between 2006 and 2012 are cited in the final text.

Acknowledgement

William Ravekes receives NIH funding (NIH NHLBI Contract HHSN268201000048C / N01-HV-08238).

References

1. Benavidez OJ, Gauvreau K, Jenkins KJ, Geva T (2008) Diagnostic errors in pediatric echocardiography: development of taxonomy and identification of risk factors. Circulation 117: 2995-3001.
2. Sheehan F, Redington A (2008) The right ventricle: anatomy, physiology and clinical imaging. Heart 94: 1510-1515.
3. Redington AN (2006) Physiopathology of right ventricular failure. Semin Thorac Cardiovasc Surg Pediatr Card Surg Annu 3-10.
4. Sengupta PP, Korinek J, Belohlavek M, Narula J, Vannan MA, et al. (2006) Left ventricular structure and function: basic science for cardiac imaging. J Am Coll Cardiol 48: 1988–2001.
5. Sutherland GR, Stewart MJ, Groundstroem KW, Moran CM, Fleming A, et al. (1994) Color Doppler myocardial imaging: a new technique for the assessment of myocardial function. J Am Soc Echocardiogr 7: 441-458.
6. Eidem BW, McMahon CJ, Cohen RR, Wu J, Finkelshteyn I, et al. (2004) Impact of cardiac growth on Doppler tissue imaging velocities: a study in healthy children. J Am Soc Echocardiogr 17: 212-221.
7. Vinereanu D, Ionescu AA, Fraser AG (2001) Assessment of left ventricular long axis contraction can detect early myocardial dysfunction in asymptomatic patients with severe aortic regurgitation. Heart 85: 30-36.
8. Weidemann F, Herrmann S, Stork S, Niemann M, Frantz S, et al. (2009) Impact of myocardial fibrosis in patients with symptomatic severe aortic stenosis. Circulation 120: 577-584.
9. Kiraly P, Kapusta L, Thijssen JM, Daniels O (2003) Left ventricular myocardial function in congenital valvar aortic stenosis assessed by ultrasound tissue-velocity and strain-rate techniques. Ultrasound Med Biol 29: 615-620.
10. Wahl A, Praz F, Schwerzmann M, Bonel H, Koestner S, et al. (2011) Assessment of right ventricular systolic function: comparison between cardiac magnetic resonance derived ejection fraction and pulsed-wave tissue Doppler imaging of the tricuspid annulus. Int J Cardiol 151: 58-62.
11. Eyskens B, Ganame J, Claus P, Boshoff D, Gewillig M, et al. (2006) Ultrasonic strain rate and strain imaging of the right ventricle in children before and after percutaneous closure of an atrial septal defect. J Am Soc Echocardiogr 19: 994-1000.
12. Vogel M, Sponring J, Cullen S, Deanfield JE, Redington AN (2001) Regional wall motion and abnormalities of electrical depolarization and repolarization in patients after surgical repair of tetralogy of Fallot. Circulation 103: 1669-1673.
13. Frommelt PC, Sheridan DC, Mussatto KA, Hoffmann GM, Ghanayem NS, et al. (2007) Effect of shunt type on echocardiographic indices after initial palliations for hypoplastic left heart syndrome: Blalock-Taussig shunt versus right ventricle-pulmonary artery conduit. J Am Soc Echocardiogr 20: 1364-1373.
14. Friedberg MK, Silverman NH, Dubin AM, Rosenthal DN (2007) Mechanical dyssynchrony in children with systolic dysfunction secondary to cardiomyopathy: a Doppler tissue and vector velocity imaging study. J Am Soc Echocardiogr 20: 756-763.
15. Labombarda F, Blanc J, Pellissier A, Stos B, Gaillard C, et al. (2009) Health-e-Child project: mechanical dyssynchrony in children with dilated cardiomyopathy. J Am Soc Echocardiogr 22: 1289-1295.
16. Janousek J, Gebauer RA, Abdul-Khaliq H, Turner M, Kornyel L, et al. (2009) Cardiac resynchronisation therapy in paediatric and congenital heart disease: differential effects in various anatomical and functional substrates. Heart 95: 1165-1171.
17. Mori K, Nakagawa R, Nii M, Edagawa T, Takehara Y, et al. (2004) Pulsed wave Doppler tissue echocardiography assessment of the long axis function of the right and left ventricles during the early neonatal period. Heart 90: 175-180.
18. Kukulski T, Hubbert L, Arnold M, Wranne B, Hatle L, et al. (2000) Normal regional right ventricular function and its change with age: a Doppler myocardial imaging study. J Am Soc Echocardiogr 13: 194-204.
19. Tei C, Ling LH, Hodge DO, Bailey KR, Oh J, et al. (1995) New index of combined systolic and diastolic myocardial performance: a simple and reproducible measure of cardiac function: a study in normals and dilated cardiomyopathy. J Cardiol 26: 357-366.
20. Eidem BW, O'Leary PW, Tei C, Seward J (2000) Usefulness of the myocardial performance index for assessing right ventricular function in congenital heart disease. Am J Cardiol 86: 654-658.
21. Murase M, Ishida A, Morisawa T (2009) Left and right ventricular myocardial performance index (Tei index) in very-low-birth-weight infants. Pediatr Cardiol 30: 928-935.
22. Matter M, Abdel-Hady H, Attia G, Hafez M, Seliem W, et al. (2010) Myocardial performance in asphyxiated full-term infants assessed by Doppler tissue imaging. Pediatr Cardiol 31: 634-642.
23. Petko C, Minich LL, Everitt MD, Holubkov R, Shaddy RE, et al. (2010) Echocardiographic evaluation of children with systemic ventricular dysfunction treated with carvedilol. Pediatr Cardiol 31: 780-784.
24. Tekten T, Onbasili AO, Ceyhan C, Unal S, Discigil B (2003) Novel approach to measure myocardial performance index: pulsed-wave tissue Doppler echocardiography. Echocardiography 20: 503-510.

25. Yasuoka K, Harada K, Toyono M, Tamura M, Yamamoto F (2004) Tei index determined by tissue Doppler imaging in patients with pulmonary regurgitation after repair of tetralogy of Fallot. Pediatr Cardiol 25: 131-136.

26. Vonk MC, Sander MH, van den Hoogen FH, van Riel PL, Verheugt FW, et al. (2007) Right ventricle Tei-index: A tool to increase the accuracy of noninvasive detection of pulmonary arterial hypertension in connective tissue diseases. Eur J Echocardiogr 8: 317-321.

27. Roberson DA, Cui W (2007) Right ventricular Tei index in children: effect of method, age, body surface area, and heart rate. J Am Soc Echocardiogr 20: 764-770.

28. Cheung MM, Smallhorn JF, Redington AN, Vogel M (2004) The effects of changes in loading conditions and modulation of inotropic state on the myocardial performance index: comparison with conductance catheter measurements. Eur Heart J 25: 2238-42.

29. Schwerzmann M, Samman AM, Salehian O, Holm J, Provost Y, et al. (2007) Comparison of echocardiographic and cardiac magnetic resonance imaging for assessing right ventricular function in adults with repaired tetralogy of Fallot. Am J Cardiol 99: 1593-1597.

30. Vogel M, Derrick G, White PA, Cullen S, Aichner H, et al. (2004) Systemic ventricular function in patients with transposition of the great arteries after atrial repair: a tissue Doppler and conductance catheter study. J Am Coll Cardiol 43: 100–106.

31. Vogel M, Schmidt MR, Kristiansen SB, Cheung M, White PA, et al. (2002) Validation of myocardial acceleration during isovolumic contraction as a novel noninvasive index of right ventricular contractility: comparison with ventricular pressure-volume relations in an animal model. Circulation 105: 1693-1699.

32. Pauliks LB, Vogel M, Madler CF, Williams RI, Payne N, et al. (2005) Regional response of myocardial acceleration during isovolumic contraction during dobutamine stress echocardiography: a color tissue Doppler study and comparison with angiocardiographic findings. Echocardiography 22: 797-808.

33. Vogel M, Cheung MM, Li J, Kristiansen SB, Schmidt MR, et al. (2003) Noninvasive assessment of left ventricular force-frequency relationships using tissue Doppler-derived isovolumic acceleration: validation in an animal model. Circulation 107: 1647-1652.

34. Tayyareci Y, Nisanci Y, Umman B, Oncul A, Yurdakul S, et al. (2008) Early detection of right ventricular systolic dysfunction by using myocardial acceleration during isovolumic contraction in patients with mitral stenosis. Eur J Echocardiogr 9: 516-521.

35. Pauliks L, Pietra B, DeGroff C, Kirby K, Knudson O, et al. (2005) Non-invasive detection of acute allograft rejection in children by tissue Doppler imaging: myocardial velocities and myocardial acceleration during isovolumic contraction. J Heart Lung Transplant 24: S239- 248.

36. Cheung MM, Smallhorn JF, McCrindle BW, Van Arsdell G, Redington AN (2005) Non-invasive assessment of ventricular force-frequency relations in the univentricular circulation by tissue Doppler echocardiography: a novel method of assessing myocardial performance in congenital heart disease. Heart 91: 1338-1342.

37. Eyskens B, Weidemann F, Kowalski M, Bogaert J, Dymarkowski S, et al. (2004) Regional right and left ventricular function after the Senning operation: an ultrasonic study of strain rate and strain. Cardiol Young 14: 255–264.

38. Ganame J, Claus P, Eyskens B, Uyttebroeck A, Renard M, et al. (2007) Acute cardiac functional changes after subsequent antracycline infusions in children. Am J Cardiol 99: 974–977.

39. Giatrakos N, Kinali M, Stephens D, Dawson D, Muntoni F, et al. (2006) Cardiac tissue velocities and strain rate in the early detection of myocardial dysfunction of asymptomatic boys with Duchenne's muscular dystrophy: relationship to clinical outcome. Heart 92: 840–842.

40. Weidemann F, Eyskens B, Jamal F, Mertens L, Kowalski M, et al. (2002) Quantification of regional left and right ventricular radial and longitudinal function in healthy children using ultrasound-based strain rate and strain imaging. J Am Soc Echocardiogr 15: 20-28.

41. Joshi S, Edwards JM, Wilson DG, Wong JK, Kotecha S, et al. (2010) Reproducibility of myocardial velocity and deformation imaging in term and preterm infants. Eur J Echocardiogr 11: 44-50.

42. Pena JL, da Silva MG, Faria SC, Salemi VM, Mady C, et al. (2009) Quantification of regional left and right ventricular deformation indices in healthy neonates by using strain rate and strain imaging. J Am Soc Echocardiogr 22: 369-375.

43. Nestaas E, Støylen A, Brunvand L, Fugelseth D (2009) Tissue Doppler derived longitudinal strain and strain rate during the first 3 days of life in healthy term neonates. Pediatr Res 65: 357-362.

44. Nestaas E, Støylen A, Brunvand L, Fugelseth D (2011) Longitudinal strain and strain rate by tissue Doppler are more sensitive indices than fractional shortening for assessing the reduced myocardial function in asphyxiated neonates. Cardiol Young 21: 1-7.

45. Koopman LP, Slorach C, Hui W, Manlhiot C, McCrindle BW, et al. (2010) Comparison between different speckle tracking and color tissue Doppler techniques to measure global and regional myocardial deformation in children. J Am Soc Echocardiogr 23: 919-928.

46. Ganame J, Mertens L, Eidem BW, Claus P, D`hooge J, et al. (2007) Regional myocardial deformation in children with hypertrophic cardiomyopathy: morphological and clinical correlations. Eur Heart J 28: 2886-2894.

47. Ho CY, Carlsen C, Thune JJ, Havndrup O, Bundgaard H, et al. (2009) Echocardiographic strain imaging to assess early and late consequences of sarcomere mutations in hypertrophic cardiomyopathy. Circ Cardiovasc Genet 2: 314-321.

48. Mertens L, Ganame J, Claus P, Goemans N, Thijs D, et al. (2008) Early regional myocardial dysfunction in young patients with Duchenne muscular dystrophy. J Am Soc Echocardiogr 21: 1049-1054.

49. Ganame J, Claus P, Uyttebroeck A, Renard M, D`hooge J, et al. (2007) Myocardial dysfunction late after low-dose anthracycline treatment in asymptomatic pediatric patients. J Am Soc Echocardiogr 20: 1351-1358.

50. Eyskens B, Brown SC, Claus P, Dymarkowski S, Gewillig M, et al. (2010) The influence of pulmonary regurgitation on regional right ventricular function in children after surgical repair of tetralogy of Fallot. Eur J Echocardiogr 11: 341-345.

51. Bos JM, Hagler DJ, Silvilairat S, Cabalka A, O`Leary P, et al. (2006) Right ventricular function in asymptomatic individuals with a systemic right ventricle. J Am Soc Echocardiogr 19: 1033-1037.

52. Amundsen BH, Helle-Valle T, Edvardsen T, Torp H, Crosby J, et al. (2006) Noninvasive myocardial strain measurement by speckle tracking echocardiography: validation against sonomicrometry and tagged magnetic resonance imaging. J Am Coll Cardiol 47: 789-793.

53. Teske AJ, De Boeck BWL, Olimulder M, Prakken NH, Doevendans PAF, et al. (2008) Echocardiographic assessment of regional right ventricular function: a head-to-head comparison between 2-dimensional and tissue Doppler-derived strain analysis. J Am Soc Echocardiogr 21: 275-283.

54. Leitman M, Lysyansky P, Sidenko S, Shir V, Peleg E, et al. (2004) Two-dimensional strain-a novel software for real-time quantitative echocardiographic assessment of myocardial function. J Am Soc Echocardiogr 17: 1021-1029.

55. Kowalski M, Kowalik E, Kotlinski K, Szymański P, Kuśmierczyk M, et al. (2009) Regional left ventricular myocardial shortening in normotensive patients late after aortic coarctation repair -normal or impaired? Ultrasound Med Biol 35: 1947-1952.

56. Laser KT, Haas NA, Jansen N, Schäffler R, Palacios Argueta JR, et al. (2009) Is torsion a suitable echocardiographic parameter to detect acute changes in left ventricular afterload in children? J Am Soc Echocardiogr 22: 1121-1128.

57. Dragulescu A, Mertens LL (2010) Developments in echocardiographic techniques for the evaluation of ventricular function in children. Arch Cardiovasc Dis 103: 603-614.

58. Dong L, Zhang F, Shu X, Guan L, Chen H (2009) Left ventricular torsional deformation in patients undergoing transcatheter closure of secundum atrial septal defect. Int J Cardiovasc Imaging 25: 479-486.

59. Cheung EW, Liang XC, Lam WW, Cheung YF (2009) Impact of right ventricular dilation on left ventricular myocardial deformation in patients after surgical repair of tetralogy of fallot. Am J Cardiol 104: 1264-1270.

60. Kutty S, Deatsman SL, Russell D, Nugent ML, Simpson PM, et al. (2008) Pulmonary valve replacement improves but does not normalize right ventricular mechanics in repaired congenital heart disease: a comparative assessment using velocity vector imaging. J Am Soc Echocardiogr 21: 1216-1221.

61. Moiduddin N, Asoh K, Slorach C, Benson LN, Friedberg MK (2009) Effect of transcatheter pulmonary valve implantation on short-term right ventricular function as determined by two-dimensional speckle tracking strain and strain rate imaging. Am J Cardiol 104: 862-867.

62. Giusca S, Dambrauskaite V, Scheurwegs C, D'hooge J, Claus P, et al. (2010) Deformation imaging describes right ventricular function better than longitudinal displacement of the tricuspid ring. Heart 96: 281-288.

63. Puwanant S, Park M, Popović ZB, Tang WH, Farha S, et al. (2010) Ventricular geometry, strain, and rotational mechanics in pulmonary hypertension. Circulation 121: 259-266.

64. Kittipovanonth M, Bellavia D, Chandrasekaran K, Villarraga HR, Abraham TP, et al. (2008) Doppler myocardial imaging for early detection of right ventricular dysfunction in patients with pulmonary hypertension. J Am Soc Echocardiogr 21: 1035-1041.

65. Becker M, Bilke E, Kuhl H, Katoh M, Kramann R, et al. (2006) Analysis of myocardial deformation based on pixel tracking in two dimensional echocardiographic images enables quantitative assessment of regional left ventricular function. Heart 92: 1102-1108.

66. Cho GY, Chan J, Leano R, Strudwick M, Marwick TH (2006) Comparison of Two-Dimensional Speckle and Tissue Velocity Based Strain and Validation With Harmonic Phase Magnetic Resonance Imaging. Am J Cardiol 97: 1661-1666.

67. Hanekom L, Cho GY, Leano R, Jeffriess L, Marwick TH (2007) Comparison of two-dimensional speckle and tissue Doppler strain measurement during dobutamine stress echocardiography: an angiographic correlation. Eur Heart J 28: 1765-1772.

68. Ingul CB, Torp H, Aase SA, Berg S, Stoylen A, et al. (2005) Automated Analysis of Strain Rate and Strain: Feasibility and Clinical Implications. J Am Soc Echocardiograph 18: 411-418.

69. Hui W, Slorach C, Bradley TJ, Jaeggi ET, Mertens L, et al. (2010) Measurement of right ventricular mechanical synchrony in children using tissue Doppler velocity and two-dimensional strain imaging. J Am Soc Echocardiogr 23: 1289-1296.

70. Niemann P, Houle H, Pinho L, Broberg C, Jerosch-Herold M, et al. (2007) An offline analysis method for determining left ventricular myocardial velocity, strain, and twist from gradient-echo cine MRI images. J Cardiovasc Magn Res 9: 276-277.

71. Truong UT, Li X, Broberg CS, Houle H, Schaal M, et al. (2010) Significance of Mechanical Alterations in Single Ventricle Patients on Twisting and Circumferential Strain as Determined by Analysis of Strain from Gradient Cine Magnetic Resonance Imaging Sequences. Am J Cardiol 105: 1465–1469.

72. Ortega M, Triedman JK, Geva T, Harrild DM (2011) Relation of Left Ventricular Dyssynchrony Measured by Cardiac Magnetic Resonance Tissue Tracking in Repaired Tetralogy of Fallot to Ventricular Tachycardia and Death. Am J Cardiol 107: 1535–1540.

73. Hor KN, Gottliebson WM, Carson C, Wash E, Cnota J, et al. (2010) With Harmonic Phase Imaging Analysis Comparison of Magnetic Resonance Feature Tracking for Strain Calculation. J Am Coll Cardiol Img 3: 144-151.

74. Simpson JM (2008) Real-time three-dimensional echocardiography of congenital heart disease using a high frequency paediatric matrix transducer. Eur J Echocardiogr 9: 222-224.

75. Friedberg MK, Su X, Tworetzky W, Soriano BD, Powell AJ, et al. (2010) Validation of 3D echocardiographic assessment of left ventricular volumes, mass, and ejection fraction in neonates and infants with congenital heart disease: a comparison study with cardiac MRI. Circ Cardiovasc Imaging 3: 735-742.

76. Soriano BD, Hoch M, Ithuralde A, Geva T, Powell AJ, et al. (2008) Matrix-array 3-dimensional echocardiographic assessment of volumes, mass, and ejection fraction in young pediatric patients with a functional single ventricle: a comparison study with cardiac magnetic resonance. Circulation 117: 1842-1848.

77. Takahashi K, Inage A, Rebeyka IM, Ross D, Thompson RB, et al. (2009) Real-time 3dimensional echocardiography provides new insight into mechanisms of tricuspid valve regurgitation in patients with hypoplastic left heart syndrome. Circulation 120: 1091-1098.

78. Dragulescu A, Grosse-Wortmann L, Fackoury C, Riffle S, Waiss M, et al. (2011) Echocardiographic Assessment of Right Ventricular Volumes after Surgical Repair of Tetralogy of Fallot: Clinical Validation of a New Echocardiographic Method. J Am Soc Echocardiogr 24:1191-1198.

79. Van der Zwaan HB, Geleijnse ML, Soliman OI, McGhie JS, Wiegers-Groeneweg EJ, et al. (2011) Test-retest variability of volumetric right ventricular measurements using real-time three-dimensional echocardiography. J Am Soc Echocardiogr 24: 671-679.

80. Niemann PS, Pinho L, Balbach T, Galuschky C, Blankenhagen M, et al. (2007) Anatomically oriented right ventricular volume measurements with dynamic three-dimensional echocardiography validated by 3-Tesla magnetic resonance imaging. J Am Coll Cardiol 50: 1668-1676.

81. Leibundgut G, Rohner A, Grize L, Bernheim A, Kessel-Schaefer A, et al. (2010) Dynamic assessment of right ventricular volumes and function by realtime three-dimensional echocardiography: a comparison study with magnetic resonance imaging in 100 adult patients. J Am Soc Echocardiogr 23: 116-126.

82. Van der Zwaan HB, Helbing WA, McGhie JS, Geleijnse ML, Luijnenburg SE, et al. (2010) Clinical value of realtime three-dimensional echocardiography for right ventricular quantification in congenital heart disease: validation with cardiac magnetic resonance imaging. J Am Soc Echocardiogr 23: 134-140.

83. Khoo NS, Young A, Occleshaw C, Cowan B, Zeng IS, et al. (2009) Assessments of right ventricular volume and function using three-dimensional echocardiography in older children and adults with congenital heart disease: comparison with cardiac magnetic resonance imaging. J Am Soc Echocardiogr 22: 1279-1288.

84. Grewal J, Majdalany D, Syed I, Pellikka P, Warnes CA (2010) Three-dimensional echocardiographic assessment of right ventricular volume and function in adult patients with congenital heart disease: comparison with magnetic resonance imaging. J Am Soc Echocardiogr 23: 127-133.

85. Van der Zwaan HB, Helbing WA, Boersma E, Geleijnse ML, McGhie JS, et al. (2010) Usefulness of real-time three-dimensional echocardiography to identify right ventricular dysfunction in patients with congenital heart disease. Am J Cardiol 106: 843-850.

86. Grapsa J, O'Regan DP, Pavlopoulos H, Durighel G, Dawson D, et al. (2010) Right ventricular remodelling in pulmonary arterial hypertension with three-dimensional echocardiography: comparison with cardiac magnetic resonance imaging. Eur J Echocardiogr 11: 64-73.

87. Lu X, Nadvoretskiy V, Bu L, Stolpen A, Ayres N, et al. (2008) Accuracy and reproducibility of real-time three-dimensional echocardiography for assessment of right ventricular volumes and ejection fraction in children. J Am Soc Echocardiogr 21: 84-89.

88. Grison A, Maschietto N, Reffo E, Stellin G, Padalino M, et al. (2007) Three-dimensional echocardiographic evaluation of right ventricular volume and function in pediatric patients: validation of the technique. J Am Soc Echocardiogr 20: 921-929.

89. Kjaergaard J, Svendsen JH, Sogaard P, Chen X, Nielsen HB, et al. (2007) Advanced quantitative echocardiography in arrhythmogenic right ventricular cardiomyopathy. J Am Soc Echocardiogr 20: 27-35.

90. Tamborini G, Marsan NA, Gripari P, Maffessanti F, Brusoni D, et al. (2010) Reference values for right ventricular volumes and ejection fraction with real-time three-dimensional echocardiography: evaluation in a large series of normal subjects. J Am Soc Echocardiogr 23: 109-115.

91. van der Zwaan HB, Geleijnse ML, McGhie JS, Boersma E, Helbing WA, et al. (2011) Right ventricular quantification in clinical practice: two-dimensional vs. three-dimensional echocardiography compared with cardiac magnetic resonance imaging. Eur J Echocardiogr 12: 656-664.

92. van den Bosch AE, Ten Harkel DJ, McGhie JS, Roos-Hesselink JW, Simoons ML, et al. (2006) Characterization of atrial septal defect assessed by real-time 3-dimensional echocardiography. J Am Soc Echocardiogr 19: 815–821.

93. van den Bosch AE, Ten Harkel DJ, McGhie JS, Roos-Hesselink JW, Simoons ML, et al. (2006) Feasibility and accuracy of real-time 3-dimensional echocardiographic assessment of ventricular septal defects. J Am Soc Echocardiogr 19: 7-13.

94. Takahashi K, Guerra V, Roman KS, Nii M, Redington A, et al. (2006) Three-dimensional echocardiography improves the understanding of the mechanisms and site of left atrioventricular valve regurgitation in atrioventricular septal defect. J Am Soc Echocardiogr 19: 1502–1510.

95. Hlavacek AM, Chessa K, Crawford FA, Atz A, Shirali GS (2006) Real-time three-dimensional echocardiography is useful in the evaluation of patients with atrioventricular septal defects. Echocardiography 23: 225-231.

96. Cheng TO, Xie MX, Wang XF, Wang Y, Lu Q (2004) Real-time 3-dimensional echocardiography in assessing atrial and ventricular septal defects: an echocardiographic-surgical correlative study. Am Heart J 148: 1091-1095.

97. Sadagopan SN, Veldtman GR, Sivaprakasam MC, Keeton BR, Gnanapragasam JP, et al. (2006) Correlations with operative anatomy of real time three-dimensional echocardiographic imaging of congenital aortic valvar stenosis. Cardiol Young 16: 490-494.

98. Anwar AM, Soliman O, Bosch AE, McGhie JS, Geleijnse ML, Cate FJ, et al. (2007) Assessment of pulmonary valve and right ventricular outflow tract with real-time three-dimensional echocardiography. Int J Cardiovasc Imaging 23: 167-175.

99. Bharucha T, Fernandes F, Slorach C, Mertens L, Friedberg MK (2011) Measurement of Effective Aortic Valve Area Using Three-Dimensional Echocardiography in Children Undergoing Aortic Balloon Valvuloplasty for Aortic Stenosis. Echocardiography [Epub ahead of print].

100. Valverde I, Rawlins D, Austin C, Simpson JM (2011) Three-dimensional echocardiography in the management of parachute mitral valve. Eur J Echocardiogr [Epub ahead of print].

101. Bharucha T, Ho SY, Vettukattil JJ (2008) Multiplanar review analysis of three-dimensional echocardiographic datasets gives new insights into the morphology of subaortic stenosis. Eur J Echocardiogr 9: 614-620.

102. Cui W, Gambetta K, Zimmerman F, Freter A, Sugeng L, Lang R, Roberson DA (2010) Real-time three-dimensional echocardiographic assessment of left ventricular systolic dyssynchrony in healthy children. J Am Soc Echocardiogr 23: 1153-1159.

103. Seliem MA, Fedec A, Szwast A, Farrell PE Jr, Ewing S, Gruber PJ, et al. (2007) Atrioventricular valve morphology and dynamics in congenital heart disease as imaged with real-time 3-dimensional matrix-array echocardiography: Comparison with 2-dimensional imaging and surgical findings. J Am Soc Echocardiogr 20: 869-876.

104. Friedberg MK, Silverman NH (2006) Cardiac ventricular diastolic and systolic duration in children with heart failure secondary to idiopathic dilated cardiomyopathy. Am J Cardiol 97: 101-105.

105. Friedberg MK, Silverman NH (2006) The systolic to diastolic duration ratio in children with heart failure secondary to restrictive cardiomyopathy. J Am Soc Echocardiogr 19: 1326-1331.

106. Patel DR, Cui W, Gambetta K, Roberson DA (2009) A comparison of Tei index versus systolic to diastolic ratio to detect left ventricular dysfunction in pediatric patients. J Am Soc Echocardiogr 22: 152-158.

107. Friedberg MK, Silverman NH (2007) The systolic to diastolic duration ratio in children with hypoplastic left heart syndrome: a novel Doppler index of right ventricular function. J Am Soc Echocardiogr 20: 749-755.

108. Bellsham-Revell HR, Tibby SM, Bell AJ, Miller OI, Razavi R, et al. (2011) Tissue Doppler time intervals and derived indices in hypoplastic left heart syndrome. Eur J Echocardiogr [Epub ahead of print].

109. Sarnari R, Kamal RY, Friedberg, MK, Silverman, NH (2009) Doppler assessment of the ratio of the systolic to diastolic duration in normal children: relation to heart rate, age and body surface area. J Am Soc Echocardiogr 22: 928-932.

110. Alkon J, Humpl T, Manlhiot C, McCrindle BW, Reyes J, Friedberg MK (2010) Usefulness of the right ventricular systolic to diastolic duration ratio to predict functional capacity and survival in children with pulmonary arterial hypertension. Am J Cardiol 106: 430-436.

111. Sengupta PP, Krishnamoorthy VK, Korinek J, Narula J, Vannan MA, et al. (2007) Left ventricular form and function revisited: applied translational science to cardiovascular ultrasound imaging. J Am Soc Echocardiogr 20: 539-551.

112. Miller D, Farah MG, Liner A, Fox K, Schluchter M, Hoit BD (2004) The relation between quantitative right ventricular ejection fraction and indices of tricuspid annular motion and myocardial performance. J Am Soc Echocardiogr 17: 443-447.

113. Meluzin J, Spinarova L, Bakala J, Toman J, Krejcí J, et al. (2001) Pulsed Doppler tissue imaging of the velocity of tricuspid annular systolic motion; a new, rapid, and non-invasive method of evaluating right ventricular systolic function. Eur Heart J 22: 340-348.

114. Meluzin J, Spinarova L, Dusek L, Toman J, Hude P, Krejci J (2003) Prognostic importance of the right ventricular function assessed by Doppler tissue imaging. Eur J Echocardiogr 4: 262-271.

115. Tuller D, Steiner M, Wahl A, Kabok M, Seiler C (2005) Systolic right ventricular function assessment by pulsed wave Doppler imaging of the tricuspid annulus. Swiss Med Wkly 135: 461-468.

116. Saxena N, Rajagopalan N, Edelman K, López-Candales A (2006) Tricuspid annular systolic velocity: a useful measurement in determining right ventricular systolic function regardless of pulmonary artery pressures. Echocardiography 23: 750-755.

117. Koestenberger M, Nagel B, Ravekes W, Avian A, Heinzl B, et al. (2011) Reference Values of the Tricuspid Annular Peak Systolic Velocity in Healthy Pediatric Patients, Calculation of z-score Values, and Comparison to the Tricuspid Annular Plane Systolic Excursion. Am J Cardiol 109: 116-121.

118. Popescu B, Antonini-Canterin F, Temporelli P, Gianuzzi P, Bosimini E, et al. (2005) Right ventricular functional recovery after acute myocardial infarction: relation with left ventricular function and interventricular septum motion. GISSI-3 echo substudy. Heart 91: 484-488.

119. Koestenberger M, Nagel B, Ravekes W, Everett AD, Stueger HP, et al. (2011) Tricuspid annular plane systolic excursion (TAPSE) and right ventricular ejection fraction in pediatric and adolescent patients with tetralogy of Fallot, patients with atrial septal defect, and age-matched normal subjects. Clin Res Cardiol 100: 67-75.

120. Koestenberger M, Nagel B, Ravekes W, Everett AD, Stueger HP, et al. (2011) Systolic right ventricular (RV) function in pediatric and adolescent patients with TOF: echocardiography versus MRI. J Am Soc Echocardiogr 24: 45-52.

121. Lamia B, Teboul JL, Monnet X, Richard C, Chemla D (2007) Relationship between the tricuspid annular plane systolic excursion and right and left ventricular function in critically ill patients. Intensive Care Med 33: 2143-2149.

122. Koestenberger M, Ravekes W, Everett A, Stueger HP, Heinzl B, et al. (2009) Right ventricular function in infants, children and adolescents: Reference values of the tricuspid annular plane systolic excursion (TAPSE) in 640 healthy patients and calculation of z-score values. J Am Soc Echocardiogr 22: 715-719.

123. Lopez L, Colan SD, Frommelt PC, Ensing GJ, Kendall K, et al. (2010) Recommendations for quantification methods during the performance of a pediatric echocardiogram: a report from the Pediatric Measurements Writing Group of the American Society of Echocardiography Pediatric and Congenital Heart Disease Council. J Am Soc Echocardiogr 23: 465-495.

124. Roberson DA, Cui W, Chen Z, Madronero LF, Cuneo BF (2007) Annular and septal Doppler tissue imaging in children: normal z-score tables and effects of age, heart rate, and body surface area. J Am Soc Echocardiogr 20: 1276-1284.

125. Eidem BW, McMahon CJ, Cohen RR, Wu J, Finkelshteyn I, et al. (2004) Impact of cardiac growth on Doppler tissue imaging velocities: a study in healthy children. J Am Soc Echocardiogr 17: 212-221.

126. Forfia PR, Fisher MR, Mathai SC, Housten-Harris T, Hemnes AR, et al. (2006) Tricuspid annular displacement predicts survival in pulmonary hypertension. Am J Respir Crit Care Med 174: 1034-1041.

127. Haworth SG, Hislop AA (2009) Treatment and survival in children with pulmonary artery hypertension: the UK pulmonary hypertension service for children 2001-2006. Heart 95: 312-317.

128. Milan A, Magnino C, Veglio F (2010) Echocardiographic indexes for the non-invasive evaluation of pulmonary hemodynamics. J Am Soc Echocardiogr 23: 225-239.

129. Rydman R, Söderberg M, Larsen F, Caidahl K, Alam M (2010) Echocardiographic evaluation of right ventricular function in patients with acute pulmonary embolism: a study using tricuspid annular motion. Echocardiography 27: 286-293.

130. Cetin I, Tokel K, Varan B, Orün U, Aslamaci S (2009) Evaluation of right ventricular function by using tissue Doppler imaging in patients after repair of tetralogy of fallot. Echocardiography 26: 950-957.

131. Lopez-Candales A, Rajagopalan N, Saxena N, Gulyasy B, Edelman K, et al. (2006) Right ventricular systolic function is not the sole determinant of tricuspid annular motion. Am J Cardiol 98: 973-977.

132. Koestenberger M, Nagel B, Ravekes W, Urlesberger B, Raith W, et al. (2011) Systolic right ventricular function in preterm and term neonates: Reference values of the tricuspid annular plane systolic excursion (TAPSE) in 258 patients and calculation of z-score values. Neonatology 100: 85-92.

133. Oosterhof T, Tulevski II, Vliegen HW, Spijkerboer AM, Mulder BJ (2006) Effects of volume and/or pressure overload secondary to congenital heart disease (tetralogy of fallot or pulmonary stenosis) on right ventricular function using cardiovascular magnetic resonance and B-type natriuretic peptide levels. Am J Cardiol 97: 1051-1055.

134. Kjaergaard J, Petersen CL, Kjaer A, Schaadt BK, Oh JK, et al. (2006) Evaluation of right ventricular volume and function by 2D and 3D echocardiography compared to MRI. Eur J Echocardiogr 7: 430-438.

This article was originally published in a special issue, **Congenital Heart Disease-Recent Discoveries and Innovations** handled by Editor(s). Dr. Georg Hansmann, Children's Hospital Boston, USA; Dr. Matthias Sigler, Georg-August University Goettingen, Germany